Proc. Indian Acad. Sci. (Chem. Sci.), Vol. 102, No. August 1990, pp. 541–553.

Physico chemical investigation of fast ion conducting AgI-Ag_2SeO_4 glasses†

M C R SHASTRY and K J RAO*
Solid State and Structural Chemistry Unit, Indian Institute of Science, Bangalore 560012, India

Ms received 21 February 1990; revised 16 May 1990

Abstract. Fast ion conducting glasses in the system $xAgI$-$(1-x)Ag_2SeO_4$ ($0{\cdot}5 \leqslant x \leqslant 0{\cdot}75$), prepared by melt quenching route have been investigated in detail. Spectroscopic, thermal and electrical properties including dielectric relaxation have been studied. An attempt is made to understand the variation in these properties by using a structural unpinning model.

Keywords. AgI-Ag_2SeO_4 glasses; fast ion conducting glasses; structural unpinning model; melt quenching.

1. Introduction

AgI-Ag_2SeO_4 glasses were first investigated by Kunze (1973) in an attempt to stabilize the high temperature fast ion conducting phase of AgI (α-AgI) at ambient temperatures by modifying the iodide ion matrix with an oxyanion of similar size and shape. It was discovered that rapidly quenched melts of AgI-Ag_2SeO_4 exhibit conductivity values an order of magnitude higher than those annealed at 403 K (Minami 1980). It was thereby speculated that glass-like structures may hold the key to the attainment of high cationic mobilities in solid electrolytes. It was suggested that microscopic domains with structural arrangements similar to that in the high temperature α-phase of AgI are retained in the process of being quenched from the melt, leading to glasses with exceptionally high conductivities (Kunze 1973).

The origin of high conductivity in AgI-based glasses has been a subject of controversy. There are many reports in the literature suggesting the formation of AgI-like clusters in these glasses (Tachez *et al* 1986; Avagadro *et al* 1987; Fontana *et al* 1987). However, there are reports of failure to notice such structures as well (Borjesson *et al* 1989). A homogeneous glass of the AgI-Ag_2SeO_4 system may therefore give rise to very high values of ionic conduction due to entirely different reasons. We have shown recently (Shastry and Rao 1989a) that high ionic conductivity in AgI-based glasses arises from structural unpinning of Ag^+ ions, which is a consequence of reduction of on-site potentials due to less than formal electrical charges possessed by the ions (see later).

† Communication no. 667 from the Solid State and Structural Chemistry Unit
* For correspondence

In this paper we report a detailed investigation on $AgI\text{-}Ag_2O\text{-}SeO_3$ glass system where we have used the structural unpinning model to understand the thermal and electrical transport properties as well as dielectric relaxation. We have also examined the infrared spectra in the region of internal vibrations of $[SeO_4]^{2-}$ ions.

2. Experimental

Commercially available AR grade starting materials were used for the preparation of glasses. The oxysalt Ag_2SeO_4 was first prepared by a simple double decomposition reaction of $AgNO_3$ and Na_2SeO_4 in aqueous medium. During heating and cooling we observed a tendency for the melt to get reduced to silver. To avoid this *in-situ* reduction, a mild oxidising agent NH_4NO_3, which decomposes upon heating above 440 K, was mixed with the charge.

5 to 10 g batches of the starting materials, mixed with about 5 g of NH_4NO_3, were gradually heated and melted in quartz crucibles. The charge was initially heated slowly till the NH_4NO_3 completely melted and decomposed (as vigorous heating of NH_4NO_3 is explosive), after which the charge was heated strongly to about 723–873 K depending on the composition of the glass. The melt was homogenized by holding it at that temperature for 15–20 min. The homogeneous melt was then quenched between two steel plates maintained at liquid nitrogen temperature. Disc-shaped samples obtained were stored in evacuated, black painted desiccators as the glasses were found to be light sensitive.

Glass transition temperature (T_g), crystallization temperature (T_c) and heat capacities (C_p) have been measured using a Perkin–Elmer DSC-2B differential scanning calorimeter. T_g was first found by a plain scan. The glasses were annealed at a temperature 5–10 K lower than T_g for several hours. These annealed samples were used for further measurements.

Heat capacity measurements were carried out on 100 mg samples in hermetically sealed aluminium cups employing a heating rate of 10 K per minute. The exact T_g was noted by the extrapolation of the linear portions on either side of the 'elbow' in the heat capacity plots.

Densities of well-annealed samples, free of air bubbles, were determined by the standard pycnometric method with xylene as the displacement liquid. The values reported here are accurate to 0·005 g/cc. Molar volumes were evaluated from molecular weight and density ($V_m = M/\rho$).

Electrical conductivities of the glasses were studied both as a function of temperature (80–300 K) and frequency (0·1–100 kHz) employing a Hewlett–Packard impedance bridge, using discs of 1 cm diameter and 0·5 mm thickness. The silver coated on both sides of the sample served as the reversible electrode (Whittingham and Huggins 1971; Chandra 1981).

Dielectric behaviour of materials is normally analysed using any one of the following quantities; complex dielectric constant ε^*, complex modulus M^*, complex admittance Y^* and complex impedance Z^*. In the present investigation we have used ε^* and M^*. The relations necessary to evaluate various quantities are as follows. The dissipation factor (D) and capacitance (C) were directly read from the bridge;

$$\text{loss tangent } \tan\delta = D \times \text{frequency (in kHz)};$$

real part of the dielectric constant $\varepsilon' = Cl/\varepsilon_0 A$, where l is the thickness of the sample, A is the effective area between the electrodes and ε_0 is the permittivity of free space = $8{\cdot}854 \times 10^{-12}$ Farad/metre;

imaginary part of the dielectric constant $\varepsilon'' = \tan\delta \times \varepsilon'$;

complex electric modulus $M^* = 1/\varepsilon^*$ where, $\varepsilon^* = \varepsilon' - i\varepsilon''$;

real part of the electric modulus $M' = \varepsilon'/(\varepsilon'^2 + \varepsilon''^2)$;

imaginary part of the electric modulus $M'' = \varepsilon''/(\varepsilon'^2 + \varepsilon''^2)$.

Infrared spectra of the glass powders dispersed in KBr pellets were recorded on a Perkin–Elmer 580 IR spectrophotometer in the range 200–1200 cm^{-1}. Pelletising and recording were done within a short period of time of about 3 min to minimize interdiffusion of K^+ ions causing significant shifts in the spectral positions.

3. Results

3.1 *Thermal properties*

The region of glass formation observed in the present investigation is shown in a ternary constitutional diagram, AgI-Ag_2O-SeO_3 in figure 1. The tie-line compositions in the ternary correspond to the pseudobinary AgI-Ag_2SeO_4 compositions. Heat capacity plots for the various compositions in the system are shown in figure 2. The glass transition temperature T_g, crystallization temperatures T_c, heat capacity (20 K below T_g) C_p, change in the heat capacity at T_g, ΔC_p, and Dulong–Petit values of heat capacities calculated assuming the tetrahedral $[SeO_4]^{2-}$ anions as single entities are all given in table 1.

The variation of ΔC_p as a function of composition is different from what one would expect because AgI-rich glasses are significantly more ionic, and hence ΔC_p should be generally high for them as is observed in many glass systems (Angell and Sichina 1976; Parthasarathy *et al* 1983). An opposite trend is observed in the present case. ΔC_p of the hypothetical AgI glass can be obtained by extrapolation in a suitable ΔC_p-composition plot (not shown) towards 100% AgI. The extrapolated value of ΔC_p

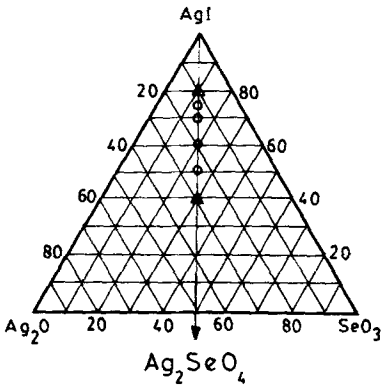

Figure 1. Glass formation region in the system AgI-Ag_2SeO_4.

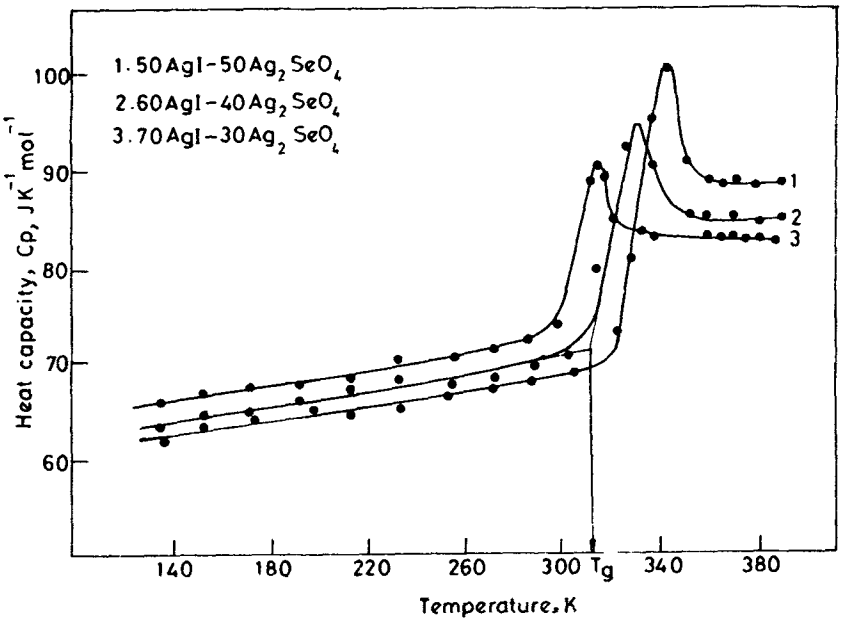

Figure 2. Variation of heat capacity with temperature for the glasses in the system $AgI\text{-}Ag_2SeO_4$.

Table 1. Glass transition temperatures, heat capacity values and the d.c. conductivity activation energies of the glasses in the system $AgI\text{-}Ag_2SeO_4$.

Composition	T_g (K)	C_p ($JK^{-1}mol^{-1}$)	ΔC_p ($JK^{-1}mol^{-1}$)	$3nR$ ($JK^{-1}mol^{-1}$)	E_a (eV)	Configurational heat capacity ($JK^{-1}mol^{-1}$)
$AgI:Ag_2SeO_4$						
50:50	327	67	19	62·3	0·28	7·0
60:40	310	69	16	59·9	0·26	13·1
70:30	295	70	17	57·4	0·23	15·0

is found to be rather low, as in a covalent glass. The origin of this behaviour will be discussed later. Glass transition temperatures decrease with increase in the mole percent of AgI. A plot of T_g as a function of mole percent of AgI in $AgI\text{-}Ag_2SeO_4$ (pseudobinary) glasses is shown in figure 3. The extrapolation of the trend towards 100% AgI gives the T_g of the hypothetical AgI glass. We have shown elsewhere (Shastry and Rao 1989a) that the T_g so determined does not compare with similarly extrapolated values for the other fast ion conducting glass systems, indicating that structural arrangement of Ag^+ and I^- ions in various AgI-based glasses may not be the same. Indeed, this feature in itself clearly demonstrates that there may not be any AgI clusters in these glasses. Further, the extrapolated T_g is less than 0·4 T_m, where T_m is the melting temperature of crystalline AgI which is too low for any good glass former (Rao 1979, 1984). Thus we infer that pure AgI glass is difficult to form and at the same time extrapolated ΔC_p values are low as in good covalent glasses. We

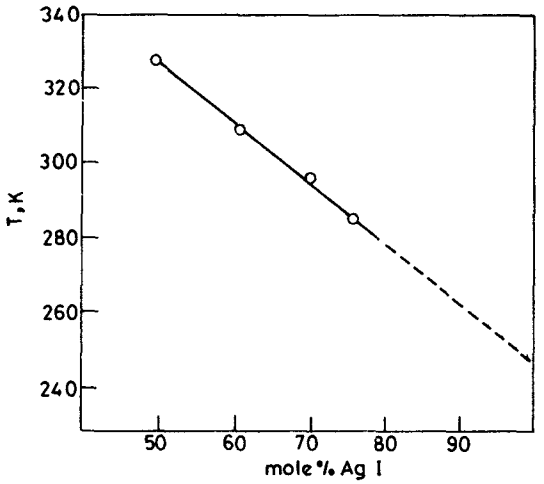

Figure 3. Variation of the glass transition temperature for the glasses in the system AgI-Ag_2SeO_4 as a function of mol% AgI.

therefore feel that the usual directional covalency of bonding may not be present in such AgI glasses in general.

Heat capacities just below T_g are uniformly higher than the Dulong–Petit value and increase with the concentration of AgI. It is as high as 15% in the case of glass containing 70% AgI. Such excess heat capacities arise from configurational entropies of glasses indicating that even in the glassy state many configurations are either frozen in or accessed as a consequence of the mobility of Ag^+ ions.

3.2 *Electrical properties*

Variation of d.c. conductivities for three compositions of AgI-Ag_2SeO_4 glasses are presented in figure 4 as Arrhenius plots. Values of log(σ) at 298 K are separately plotted in figure 5 as a function of AgI concentration. Included in figure 5 is the literature value of $\sigma_{298\,K}$ for a 75% AgI glass. The activation energies decrease with increasing AgI content, while the conductivity increases. The variation also suggests that it levels off at higher concentrations of AgI. The temperature variation of a.c. conductivity of 50 AgI-50 Ag_2SeO_4 glass is presented in figure 6 for various frequencies as Arrhenius plots. There is clearly an increase in the activation barriers at lower frequencies. The extrapolated values of E_a for zero frequency (d.c. value) from the a.c. conductivity plots are consistent with the activation barriers determined from plotting 'zero frequency values' of conductivity as a function of temperature.

Dependence of ε' is shown as a function of frequency at various temperatures in figure 7. Variation of log (tan δ) as a function of temperature is shown at various frequencies in figure 8. There is a gradual shift in the temperatures of loss peak as the frequencies of measurements increase. Given in the inset to figure 8 is the log–log plot of ε'' as a function of frequency at various temperatures. The (ε', ε'') data were converted to (M', M'') data and the behaviour of M' and M'' as a function of log (frequency) are shown in figures 9 and 10 respectively, for the 50 AgI-50 Ag_2SeO_4 glass. The variation of M' exhibits the usual sigmoidol behaviour and in all cases tends

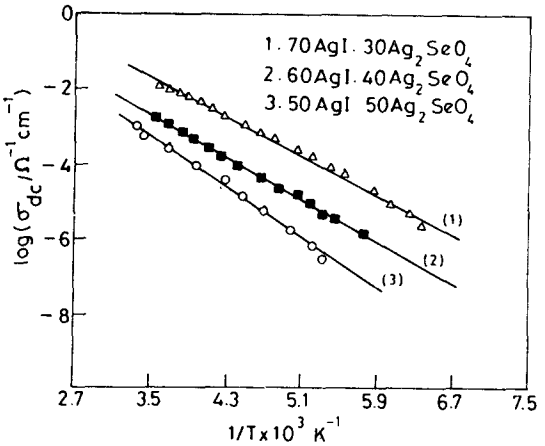

Figure 4. Variation of the d.c. conductivity with temperature for the glasses in the system $AgI\text{-}Ag_2SeO_4$.

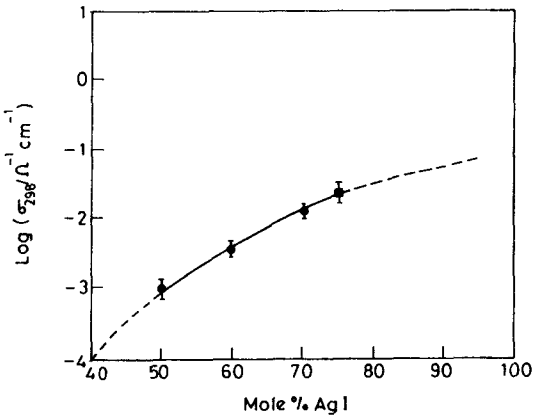

Figure 5. Variation of the conductivity at 298 K with mol% AgI for the glasses in the system $AgI\text{-}Ag_2SeO_4$.

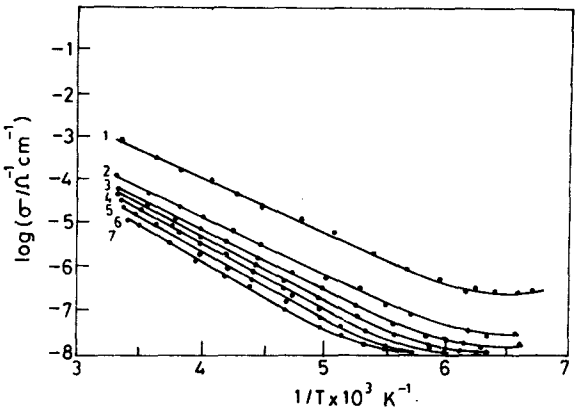

Figure 6. Variation of the a.c. conductivity with temperature at different frequencies for the glass $50AgI\text{-}50Ag_2SeO_4$. Numbers 1–7 correspond to frequencies (in kHz) 100, 30, 10, 3, 1, 0·3 and 0·1, respectively.

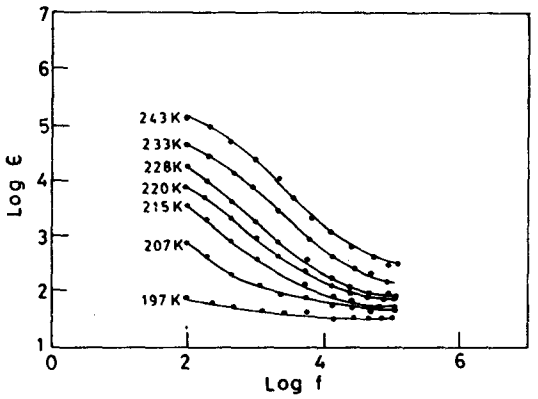

Figure 7. Variation of the real part of the dielectric constant (ε') with frequency for the glass $50AgI\text{-}50Ag_2SeO_4$.

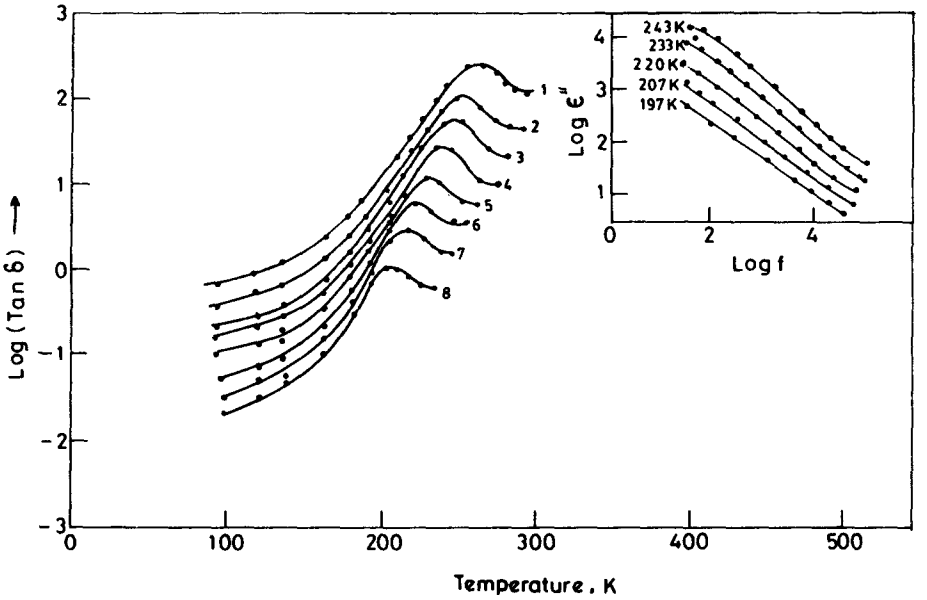

Figure 8. Variation of the loss angle with temperature for the glass $50AgI\text{-}50Ag_2SeO_4$. Numbers 1–8 correspond to frequencies (in kHz) 100, 50, 30, 10, 3, 1, 0·3, and 0·1, respectively. Inset: variation of the imaginary part of the dielectric constant (ε'') for the same glass.

towards zero at lower frequencies due to inherently large conductivities of these materials (leading to large ε'', figure 7). M'' values exhibit well-defined broad relaxation peaks in the frequency regime of our measurements in the temperature range of 180–220 K. The width of the loss peaks ($\sim$ 2·5 decades) is approximately 1·5 decades higher than that expected from a simple Debye dielectric (which is generally 1·3 decades). In figure 11, a plot of $M''/M''_{(max)}$ vs $\log(f/f_{(max)})$ is presented, which shows that the imaginary part of the modulus relaxes similarly at all temperatures. Activation energy determined from a plot of $\log(f_{(max)})$ vs. $1/T$ (0·29 eV) agrees very well with

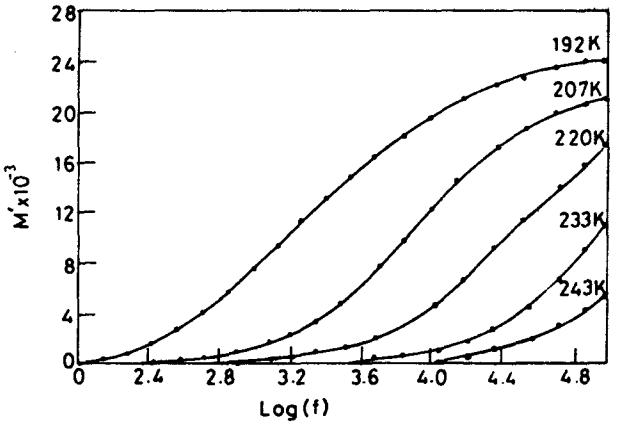

Figure 9. Variation of the real part of the electric modulus (M') with frequency at different temperatures for the glass 50AgI-50Ag_2SeO_4.

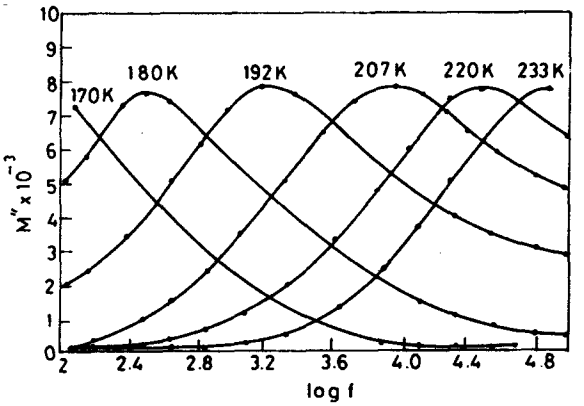

Figure 10. Variation of the imaginary part of the electric modulus (M'') with frequency at different temperatures for the glass 50AgI-50Ag_2SeO_4.

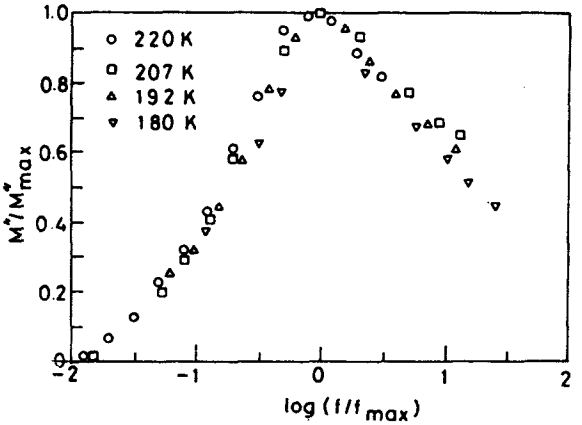

Figure 11. Plot of normalized M'' against normalized frequency for the glass 50AgI-50Ag_2SeO_4.

Table 2. The SUN (S) and other physical properties of the glasses in the system AgI-Ag_2SeO_4.

Composition	Average electro-negativity	N_{Ag} (mol^{-1})	density (g/cc)	Molar volume (cc)	Effective volume available for Ag^+ ions (cc)	S $\times 10^2$	$\sigma_{25°C}$ ($mho\,cm^{-1}$) ($\times 10^{-3}$)	T_g (K)	T_c (K)
AgI : Ag_2SeO_4									
50:50	1·241	1·50	6·451	46	16·9	0·91	0·94	327	387
60:40	1·028	1·40	6·463	44	16·3	1·13	0·40	310	347
70:30	0·816	1·30	6·475	42	15·7	1·47	9·4	295	380
75:25	0·719	1·25	6·644	40	14·5	1·67	1·0	283	347

the d.c. values discussed earlier. The M'' – log f plot was analysed using a stretched exponential relaxation function

$$\phi(t) = \phi_0 \exp[-(t/\tau)^{\beta}], \tag{1}$$

where β is the stretching exponent. Determination of β has been described in the literature (Moynihan *et al* 1973). Briefly, in order to determine β, M' vs ln f plots (figure 9) are used to determine the high frequency limiting value of M' namely, M_s. Using M_s in the relation $N^*(\omega) = [M^*(\omega)/M_s] + 1$, $N^*(\omega)$ is obtained. This is followed by evaluation of real and imaginary parts of $N^*(\omega)$ [namely, $N'(\omega)$ and $N''(\omega)$]. The real and imaginary parts of the relaxation function $N^*(\omega)$, are then plotted as a function of log(frequency) to obtain the maximum value of $N''(\omega)$ ($= N''_m$) and the full width at half maximum, Δ, of $N''(\omega)$. Using the Δ values so determined together with the data provided in the literature (table 2, Moynihan *et al* 1973), β value is determined by interpolation (for more accurate values a finer grid of β vs Δ was obtained and interpolation was carried out).

3.3 *Dielectric relaxation and structural unpinning model*

We have noted that the conductivity increases as a function of AgI concentration and the dielectric behaviour is that of a lossy dielectric obeying stretched exponential type of relaxation. All this is consistent with the model of structural unpinning in AgI-based fast ion conducting glasses. Briefly, the structural unpinning model considers that silver ions in AgI-based fast ion conducting glasses are relatively free – unpinned from their potential wells – due to a combination of (i) high unscreened nuclear charge of the Ag^+ cation, (ii) low on-site electronegativity of the anion, and (iii) available structural volume for the transport of cations. As a consequence of factors (i) and (ii), part of the charge is transferred from the anion matrix to the cations decreasing the on-site effective charge of Ag^+ ions as contrasted to its formal charge of unity. The anion matrix consists of I^- and $[SeO_4]^{2-}$ ions and their effective electronegativity may be taken as the weighted average or geometric mean of the electronegativities of individual anions. We have used the weighted average values of electronegativity. The available structural volume for the cations is given by $V_m - \Sigma V_{anions}$ divided by the total number of Ag^+ ions in the glass, $[Nf(AgI) + 2N(1-f)Ag_2SeO_4) = N(2-f)]$, where N is the Avagadro number. We have shown elsewhere (Shastry and Rao 1989a) that σ can be expressed as

$$\sigma = \sigma_0[1 - e^{-aS}]^{-1}, \tag{2}$$

where a is a constant and $S = C\cdot(Z^*/\chi_{av})\,(V_m/N)$ is the structural unpinning number, SUN. C is simply $1{\cdot}0\,\mathrm{cm}^{-3{\cdot}5}$, a constant that renders S nondimensional. Z^*, χ_{av}, V_m and N are the unscreened nuclear charge, average electronegativity, molar volume and the total number of Ag^+ ions per mole respectively. The lower on-site charges on cations and anions decrease the interaction potentials, rendering the potential wells in which Ag^+ ions are located shallow. This has the effect of lowering the potential barrier for transport and hence there is an increase in conductivity. Using $\sigma_0 = 5 \times 10^{-2}\,\mathrm{mho\,cm}^{-1}$ and $a = 3{\cdot}3 \times 10^{-3}$ the solid line shown in figure 5 was obtained indicating an excellent fit to the observed data. C could be absorbed into a, in which case a will have units of $\mathrm{cm}^{-3{\cdot}5}$.

Equation (2) rationalizes the important observation that the conductivity does not increase much after a concentration of about 70% AgI in the glasses. Further, anions which have the lowest χ are the most effective in inducing fast ion conduction; $[SeO_2]^{-2}$ is one such ion while I^- ions possess the lowest χ. AgI is thus the best candidate among inorganic silver salts for making fast ion conductors. In (2) V_m can also be exploited for making good fast ion conductors by making glasses containing borates or phosphates which tend to form open structures.

It may be noted that in the model there is no need to assume that different types of Ag^+ ions are present in the glass structure. However, ionic glasses often consist of cluster-tissue texture. When the glass forming melt is supercooled cluster-tissue texture develops in an effort to optimize the configurational entropy of the supercooled melt (Rao 1979, 1984; Rao and Rao 1982; Parthasarathy *et al* 1983). The presence of cluster-tissue texture affects transport only to the extent that it makes V_m slightly different and does not affect the functional form suggested above. In (2), the constant a can be obtained from log(activation energy) vs S plots using the following arguments. Since S is generally high for fast ion conducting glasses (Shastry and Rao 1989a) we may write (2) as,

$$\ln\sigma \simeq \ln\sigma_0(1 + e^{-aS}),$$

where, σ_0 is the conductivity of the hypothetical AgI glass. We make an approximation that this σ_0 is the same for all AgI-based glasses and use the high temperature limiting conductivity σ_0 obtained from AgI glasses. (We emphasize that this is not essential, we only need an assumed temperature independent value of σ_0. But by this assumption we can obtain some simple approximations.) We then compare $\ln\sigma$ from (2) and $\ln\sigma$ from the conventional Arrhenius equation

$$\sigma = \sigma_0 e^{-E/RT},$$

and write

$$-E_a/RT = \ln\sigma_0 e^{-aS}.$$

We then have

$$-\ln E_a = aS - [\ln\ln(1/\sigma_0) + \ln RT] \tag{3}$$

Hence a plot of $\ln E_a$ vs. S can be used to determine a.

We can also evaluate the pressure dependence of conductivity expected from the

structural unpinning model. Differentiating (2) with respect to pressure we have

$$\frac{d(\ln \ln \sigma)}{dP} = \frac{d(\ln \ln \sigma_0)}{dP} - \frac{ae^{-aS}}{1+e^{-aS}}\left(\frac{dS}{dP}\right).$$

Since

$$\frac{dS}{dP} = \frac{CZ^*}{\chi_{av}}\frac{1}{N}\left(\frac{dV_m}{dP}\right) = -\frac{CZ^*}{N}\frac{V_m}{\chi_{av}}\left(-\frac{1}{V_m}\frac{dV_m}{dP}\right) = -S\kappa,$$

where κ is the compressibility, we have

$$\frac{d(\ln \ln \sigma)}{dP} = \frac{d(\ln \ln \sigma_0)}{dP} + \frac{ae^{-}aS}{1+e^{-aS}}S\kappa. \tag{5}$$

Thus when κ is sufficiently high the sign of $d(\ln \ln \sigma)/dP$ can be positive. Indeed, in glasses where cluster-tissue textures exist, κ is initially high because the more compressible tissue dominates the pressure response at low P values. When all the tissue is converted into cluster-like structure under pressure, κ decreases and hence conductivity decreases upon further increase of pressure (Hemlata *et al* 1983).

3.4 *General consideration*

We have whown elsewhere (Parthasarathy *et al* 1983; Rao 1984) that in the cluster model of glass transition, whenever the inter-particle interaction potentials decrease and the potential wells become shallow, T_g decreases because of the decrease in the vibrational excitation energy to which T_g is directly related. When the proportion of AgI increases in the glass, S increases achieving precisely the requirement for lowering T_g as observed here because the interaction potentials weaken as a consequence of decrease of effective charge on ions.

Another important consequence of reduction of charge on anions is the weak bonding which can occur between $[SeO_4]^{(2-\delta)}$ ions. The nonbonding p orbitals of oxygen are involved in the reverse charge transfer. Such anions are now capable of overlapping with either $I^{(1-\delta)}$ or similar orbitals of other $[SeO_4]^{(2-\delta)}$ ions. A schematic MO diagram for $[SeO_4]^{2-}$ ions is shown in figure 12. It is evident that bonding orbitals are unaffected. Hence no shifts are observed in the IR spectra in the region of internal vibrations of $[SeO_4]^{2-}$ ions (figure 13). However, additional absorption features develop in AgI-rich compositions on either side of the 875 cm^{-1} stretching band. We may attribute these features to lowering of symmetry of $[SeO_4]^{2-}$ ions from T_d to C_{3v} due to the weak bonding discussed above which gives rise to new IR active vibrations. Direct NMR evidence for reverse charge transfer in AgI-$AgPO_3$ glasses has been published elsewhere earlier (Shastry and Rao 1989c).

Structural unpinning creates shallow potential wells which allow extensive inter-cation interactions which, we suggest, give rise to large densities of state of low excitation energy. This is perhaps the origin of correlated states (Shastry and Rao 1989b). It has been argued in the literature that correlated states can give rise to both power law and stretched exponential (Ngai and White 1979; Ngai *et al* 1984) behaviour of dielectric relaxation. Hence the observed relaxation behaviour in M'' vs. $\log f$ of figure 10 is expected to be quite consistent with the structural unpinning concept.

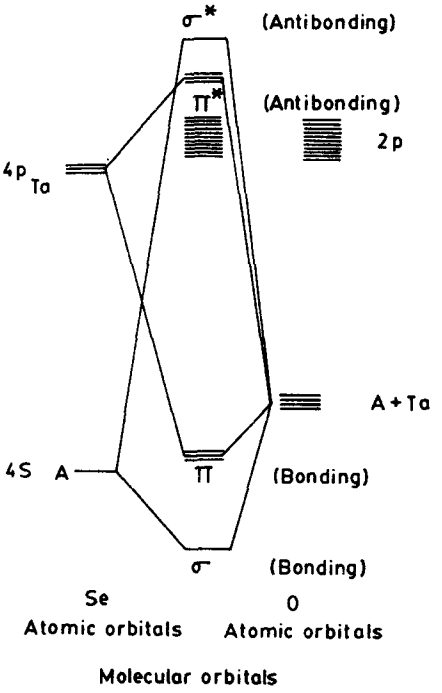

Figure 12. Schematic representation of the molecular orbital (MO) diagram of the $[SeO_4]^{2-}$ ion.

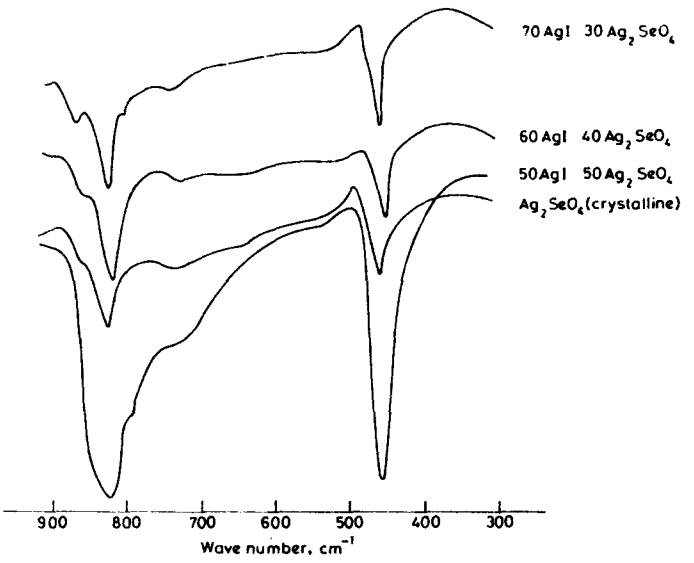

Figure 13. Infrared spectra of glasses in the system AgI-Ag_2SeO_4 along with the crystalline Ag_2SeO_4.

The β value of 0·55 observed for selenates further suggests that the disordering of Ag^+ ions in the glasses is quite extensive.

4. Conclusions

Variation of d.c. electrical conductivity, T_g, heat capacity and IR spectroscopic features in fast ion conduction in AgI-Ag_2SeO_4 glasses are shown to be consistent with the structural unpinning model. It has been suggested that the observed dielectric relaxation is related to the structural unpinning and altered ion interactions in these glasses.

Acknowledgment

The authors are thankful to Prof. C N R Rao for his kind encouragement.

References

Angell C A and Sichina W 1976 *Ann. N. Y. Acad. Sci.* **279** 53
Avagadro A, Aldrovandi S, Borsa F and Carini G 1978 *Philos. Mag.* **B56** 227
Borjesson L, Torrel L M and Howells W S 1989 *Philos. Mag.* **B59** 105
Chandra S 1981 in *Superionic solids: principles and applications* (Amsterdam: North-Holland) p. 148
Kunze D 1973 in *Fast ion transport in solids* (ed) W VanGool (Amsterdam: North-Holland) p. 405
Fontana A, Rocca F and Fontana M P 1987a *Phys. Rev. Lett.* **58** 503
Fontana A, Rocca F and Fontana M P 1987b *Philos. Mag.* **B56** 251
Hemlata S, Parthasarathy G, Lakshmikumar S T and Rao K J 1983 *Philos. Mag.* **B47** 291–297
Minami T, Imazoa K and Tanaka M 1980 *J. Non-Cryst. Solids* **42** 469
Moynihan C T, Boesh L P and Laberge N L 1973 *Phys. Chem. Glasses* **14** 122
Nagi K L, Rendell R W and Jain H 1984 *Phys. Rev.* **B30** 2133
Ngai K L and Whited C T 1979 *Phys. Rev.* **B20** 2475
Parthasarathy R, Rao K J and Rao C N R 1983 *Chem. Soc. Rev.* **12** 361
Rao K J 1979 *Bull. Mater. Sci.* **1** 181
Rao K J 1984 *Proc. Indian Acad. Sci. (Chem. Sci.)* **93** 389
Rao K J and Rao C N R 1982 *Mater. Res. Bull.* **17** 1337
Shastry M C R and Rao K J 1989a *Solid State Ionics* **37** 17
Shastry M C R and Rao K J 1989b *Solid State Ionics* (communicated)
Shastry M C R and Rao K J 1989c *Pramana – J. Phys.* **32** 811
Tachez M, Mercier M, Malugani J P and Dionoux A J 1986a *Solid State Ionics* **20** 93
Tachez M, Mercier M, Malugani J P and Dionoux A J 1986b *Solid State Ionics* **18/19** 421
Whittingham M S and Huggins R A 1971 *J. Chem. Phys.* **54** 414